

# Mutual correlation of sol-gel optical properties and repeatability of production process examined by statistical pattern recognition methods

JOANNA KOBEL, HALINA PODBIELSKA, MONIKA LECHNA-MARCZYŃSKA, AGNIESZKA ULATOWSKA-JARŻA

Institute of Physics, Bio-Optics Group, Wrocław University of Technology, Wybrzeże Wyspiańskiego 27, 50-370 Wrocław, Poland, e-mails: jkobel@if.pwr.wroc.pl, Halina.Podbielska@pwr.wroc.pl.

The methods based on the statistical pattern recognition are used for the evaluation of microscopic images of sol-gel matrices. The applied classification is a two steps scheme: dimensionality reduction of the data and cluster analysis. The obtained results have demonstrated that the molar ratio  $R$  (the number of solvent moles to the number of substrate moles) influences the stability of sol-gel materials, thus enabling us to reach the higher repeatability of the production process. It has been shown that the repeatability varies between 96.67% (for molar ratio  $R = 5$ ) and 98.33% (for  $R = 15, 32, 50$ ). This corresponds with the results of light scattering and transmission measurements.

Keywords: sol-gel matrix, physical properties, repeatability of production, pattern recognition, dimensionality reduction, cluster analysis.

## 1. Introduction

Sol-gel matrices belong to the group of porous materials [1]. The porosity is defined as the fraction of pores volume to the total volume. Generally, porous materials have the porosity of 0.2–0.95.

The broad range of possible applications of sol-gel derived materials has marked this technology as one of the most promising fields of contemporary material sciences [2]–[5]. The sol-gel materials can be used for the construction of various optoelectronic devices, including optodes of optical sensors. The performance of such devices is connected with sol-gels thermal and chemical stability, transparency, as well as their porosity, which facilitates the transport of gases or liquids through the material. Therefore, the structure of matrices is so important as their optical properties.

The sol-gel production process leads to the formation of gel from mixtures of liquid reagents after hydrolysis at ambient temperatures. It involves several steps: the evolution of inorganic networks, formation of colloidal suspension (sol) and gelation of the sol to form a network in a continuous liquid phase (gel). Drying of the obtained gels, even at room temperatures, leads to the formation of glass-like materials called xerogels – porous, usually transparent and relatively sturdy.

The whole process is affected by the properties of the starting precursors, pH, catalyst, concentration, temperature, presence or absence of salts and additives, aging and drying conditions. Molar ratio  $R$  (denoting the number of solvent moles to the number of precursor moles), pH and drying conditions are ones of the most important variables that can affect the gel pore structure.

Controlling the physical and chemical parameters of production process yields materials with precisely tailored parameters such as mechanical strength, transparency, size and distribution of the pores network [6]. For the practical applications, one has to be able to produce the material with high repeatability. As it was mentioned, the production process is quite sensitive to several factors, so even under the same conditions it is difficult to obtain the same properties of final product.

In this work we check the repeatability of sol-gel process by analyzing the microscopic images of sol-gel films produced with various molar ratios  $R = 5, 15, 32$  and  $50$ . For that purpose the statistical pattern recognition methods were used. The number of well recognized images testifies to the repeatability of sol-gel production process. The repeatability was then compared to the optical properties such as refractive index and VIS transmittance.

## 2. Materials

The examined sol-gel matrices were produced from silica based precursors in the form of  $1\ \mu\text{m}$  thick single layers deposited on microscopic glasses. The suitable amount of solvent (we used ethyl alcohol) was added during the hydrolysis process, so thus to obtain the required molar ratio  $R$ . First, the silicate precursor tetraethoxysilan (TEOS  $\text{Si}(\text{OC}_2\text{H}_5)_4$ , 98% from Aldrich) was mixed with water and catalyst (HCl) and stirred for 4 hours by means of a magnetic stirrer. For high quality layers the addition of detergent is required. In this study the Triton X-100 (from Aldrich) was used. After the hydrolysis the pH of the obtained homogenous hydrolyzate was gradually brought up to  $\sim 6$  by means of a diluted ammonia solution. This step reduced the mechanical stress during the drying and prevented, to some extent, the risk of the sample cracking. Next, the corresponding amount of the mixture was spread onto the glass plates with a clean glass rod. Quick evaporation of the solvent led to gel formation. All examined samples produced with  $R = 5, 15, 32$  and  $50$  were stored for one month in room temperature.

## 3. Examination methods

After 1 month of aging, the samples surfaces were examined by means of an optical microscope. The CCD camera recorded the microscopic images observed on the computer monitor. The Fly Video Life View<sup>®</sup> frame grabber was used for image capturing. The images were stored in bitmap formats with resolution  $778 \times 522$  pixels.

In our experiment 80 sol-gels matrices were analyzed. The microscopic picture of each sol-gel material was examined in 6 various points represented by a randomly

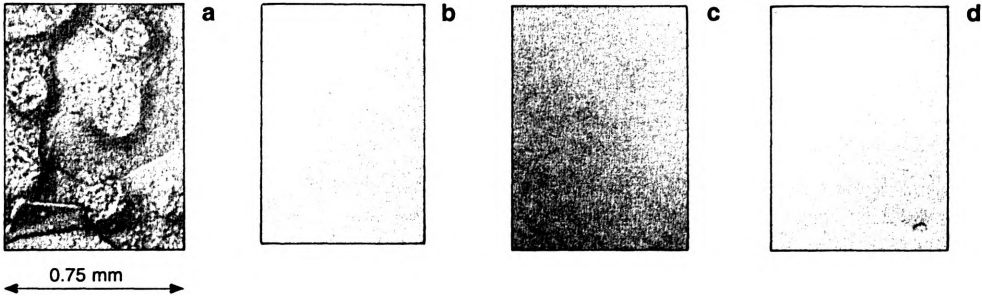


Fig. 1. Examples of microscopic pictures of tested sol-gel layers: **a** – class 1,  $R = 5$ ; **b** – class 2,  $R = 15$ ; **c** – class 3;  $R = 32$ ; **d** – class 4;  $R = 50$ .

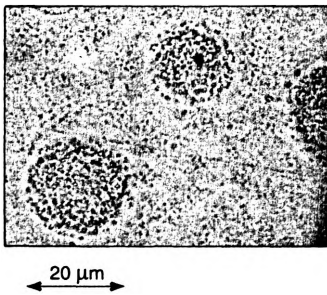


Fig. 2. Sol-gel material with well-observed density fluctuation (optical microscope),  $R = 5$ , primary and secondary aggregates are observed.

chosen sample of  $25 \times 25$  pixels, so thus the total number of examined samples was 480. Figure 1 presents exemplary images of sol-gel materials (classes) that were analyzed. Class number means that all materials in the class were produced with the same molar ratio  $R$ .

The measurements of refractive indices were performed by means of Abbe refractometry. The transmittances were measured by means of a computer aided spectrophotometer from OceanOptics. Additionally, the dimension of pores was estimated by light scattering method.

Sol-gel materials are not uniform structurally and show typical density fluctuations (see Fig. 2). The static light scattering techniques enable us to distinguish between different sizes of Si–O–Si chains aggregates [7]. The correlation length  $a_1$  and correlation length  $a_2$  represent the average size of Si–O–Si strings aggregates and average pore diameter, respectively. Parameters describing the structure of sol-gel materials can be calculated from the random density fluctuation theory [8].

According to Debye and Bueche theory, the intensity  $I(\phi)$  of light scattered by random density fluctuations can be written in the following form:

$$I(\phi) = K \int c(r) \frac{\sin(hr)}{hr} r^2 dr \quad (1)$$

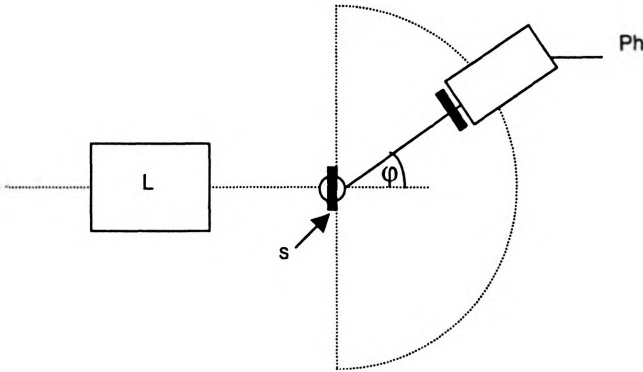


Fig. 3. Experimental set-up for light scattering measurements (L – He-Ne laser, s – sample of the sol-gel material, Ph – photomultipliers).

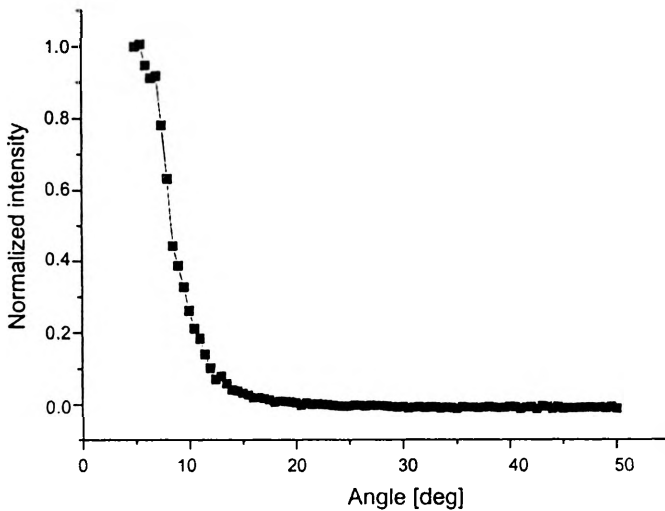


Fig. 4. Typical intensity of the light scattered by the sol-gel material as a function of scattering angle at 20 °C. The intensity measured for an angle greater than 20° does not exceed zero level.

where  $c(r)$  is the correlation function of the density fluctuation,  $h = (4\pi n/\lambda)\sin(\phi/2)$ , while  $\lambda$  is the wavelength of the light in the medium,  $\phi$  is the scattering angle,  $n$  is refractive index,  $r$  is the radius of the aggregate and  $K$  is a parameter dependent on the wavelength and the average deviation in the density fluctuation. For the sections of the sol-gel, the correlation function  $c(r)$  can be given by

$$c(r) = \sum_{i=1}^2 A_i \exp\left(\frac{-r^2}{a_i^2}\right) \quad (2)$$

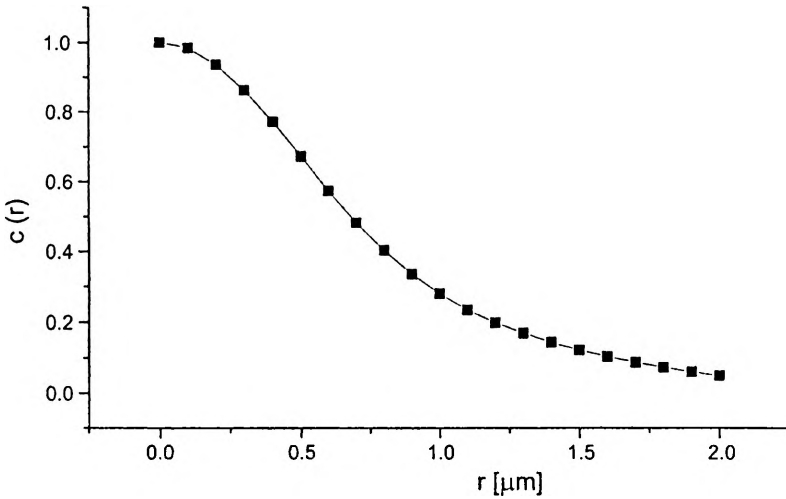


Fig. 5. Correlation function of the density fluctuation as a function of the radius of aggregates.

where the correlation lengths  $a_1$  and  $a_2$  represent diameters of the aggregates and their separation from each other, respectively, while  $A_1$  and  $A_2$  are volume fractions of the elements and

$$\sum_{i=1}^2 A_i = 1. \quad (3)$$

The scattering intensity was measured in the set-up consisting of a He-Ne laser and a photomultiplier located on a circulating arm of a goniometer, thus enabling us to measure the angles from  $5^\circ$  to  $70^\circ$  (Fig. 3). The correlation function  $c(r)$  can be evaluated from the angular dependence of the scattering intensity (*e.g.*, Fig. 4). Figure 5 shows the correlation function responsible for the density fluctuations. The correlation lengths  $a_1$  and  $a_2$  represent the radius of the aggregates (secondary particles) and their separation from each other (macropores) respectively, while the parameter  $A_i$  is the volume fraction of the elements.

#### 4. Methodology of statistical pattern recognition

For the examination of repeatability of sol-gel production process the methods based on the statistical pattern recognition were used. First, the linear discriminant analysis (LDA) [9], [10] for the feature selection and dimensionality reduction of data was exploited. LDA generated a new basis, which spanned a lower dimensional subspace than the original one, and simultaneously provided an extraction of these data features that were the most specific to different classes (in our case – different from sol-gels materials).

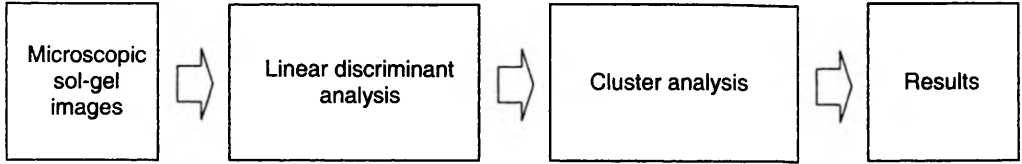


Fig. 6. Scheme of the procedure for sol-gel production process repeatability estimation.

Next, the classification based on cluster analysis was performed [11]. The scheme of the applied procedure is shown in Fig. 6.

As a measure of repeatability, percentage of well-classified images (RF – repeatability factor) was taken:

$$\text{RF} = \frac{N_{\text{wci}}}{M} \cdot 100\% \quad (4)$$

where  $N_{\text{wci}}$  is the number of well-classified images of  $i$ -th class and  $M$  is the number of samples in the  $i$ -th class.

#### 4.1. Linear discriminant analysis

The main goal of the LDA [12] is to optimize the extracted features for the purpose of classification. LDA bases on the Fisher criterion, which is a separability measure constructed by using two matrices: the within-class scatter matrix and between-class scatter matrix. These matrices are measures of scatter between classes.

In the statistical pattern recognition, objects are represented as  $N$ -dimensional vectors, so first, each  $n \times n$  pixels of sol-gel image is converted into  $n^2 = N$  element vector. Next class mean vector  $u_i$  is computed as follows:

$$u_i = \frac{1}{M} \sum_{j=1}^{M_i} x_{i,j} \quad (5)$$

where  $x_{i,j}$  is the  $j$ -th vector taken from the  $i$ -th class ( $i = 1, \dots, L, j = 1, \dots, M_i$ ),  $L$  is the number of classes, and  $M$  is the number of objects (vectors) in each class. Then mean vector, regardless of class, is calculated by formula

$$u = \sum_{i=1}^L p_i u_i \quad (6)$$

where  $p_i$  is the probability of the  $i$ -th class. Moreover, set of zero mean vectors is written as

$$\hat{x}_{i,j} = x_{i,j} - u_i. \quad (7)$$

The mentioned above the within-class scatter matrix can be defined as

$$S_w = \sum_{i=1}^L p_i C_i \quad (8)$$

where within-class correlation matrix  $C_i$  is described as

$$C_i = \frac{1}{M} \sum_{j=1}^{M_i} \hat{x}_{i,j} \hat{x}_{i,j}^T \quad (9)$$

The between-class scatter matrix is defined by

$$S_b = \sum_{i=1}^L p_i (u_i - u)(u_i - u)^T \quad (10)$$

Next the separation matrix can be calculated

$$S = S_w^{-1} S_b \quad (11)$$

and its trace, that is our measure of the discrimination power, can be maximized

$$J = \text{trace}(S). \quad (12)$$

At the end, by taking a few first eigenvectors of separation matrices, associated with maximal eigenvalues, the new reduced space is obtained [13].

## 4.2. Cluster analysis

The cluster analysis encloses a number of different classification algorithms that can organize data into relatively homogenous groups (clusters). The hierarchical clustering of  $M$  objects consists of  $M-1$  steps of successively merging clusters. At the beginning of the procedure each object is defined as an independent cluster. The algorithm merges at every step two clusters. Each of these may be one of the original objects or clusters merged at a previous step. The choice of which cluster to merge is based on a measure of the distance between pairs or clusters and decision rule. We used the Euclidean distance – probably the most commonly chosen type of measure – which is the geometric distance in the multidimensional space [14], [15].

For data classifying we applied single linkage method (also named nearest neighbours method). In this method, the distance  $d_{ab}$  between clusters  $a$  and  $b$  is determined by the closest distance between any two objects in these different clusters, as follows:

$$d_{ab} = \min(d(x_{ai}, x_{bj})) \quad (13)$$

where  $x_{ai}$  is the  $i$ -th object in the cluster  $a$ ,  $x_{bj}$  is the  $j$ -th object in the cluster  $b$ . Moreover  $i \in (1, 2, \dots, n_a)$ ,  $j \in (1, 2, \dots, n_b)$ ,  $n_a$  is the number of objects in the cluster  $a$  and  $n_b$  is the number of objects in the cluster  $b$ .

### 5. Results and conclusions

Our recent studies proved that the  $R$  ratio influences the quality of sol-gel matrices produced in the form of layers deposited on glass plates. The best results were achieved in case of samples produced on alcohol with addition of detergent and molar ratio 50, 32 and 15. Figure 7 presents the repeatability of the production of various sol-gel matrices. The highest RF reaching 98.33% is observed for sol-gel matrices from classes 2, 3 and 4. The lowest (96.67%) RF factor was for  $R = 5$ .

The results obtained from scattering measurements, transmittances and indices of refraction are presented in the Table.

As an example the measured transmittances are shown in Fig. 8. We stated that the lowest quality was observed for the sample produced with  $R = 5$ . In this case the

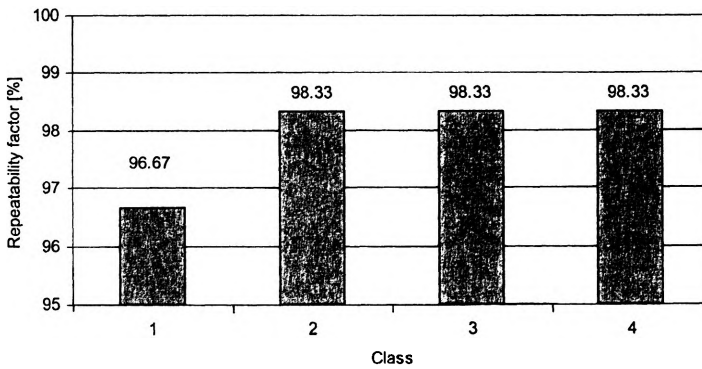


Fig. 7. Repeatability factor of examined sol-gel matrices (classes).

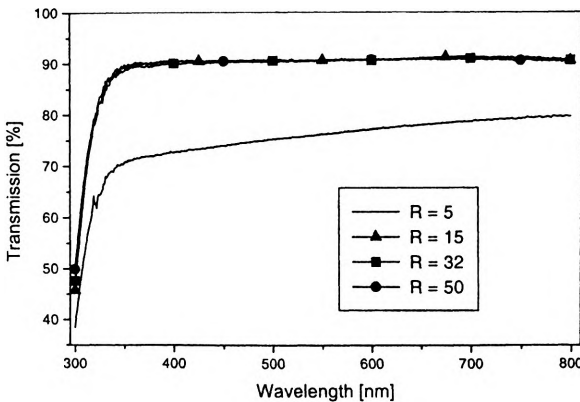


Fig. 8. Transmittance of sol-gel layers.



Table. Results of optical measurements.

Class No.	$R$	Correlation length		$n$	$T_{\max}$ [%]
		$a_1$ [ $\mu\text{m}$ ]	$a_2$ [ $\mu\text{m}$ ]		
1	5	—	—	—	70–80
2	15	1.25±0.01	0.41±0.01	1.376	90
3	32	1.81±0.01	0.76±0.01	1.388	90
4	50	1.28±0.01	0.39±0.01	1.377	90

transmittance did not exceed 80%. Due to the inhomogeneity it was impossible to measure the intensity of scattered light, thus we were not able to calculate the correlation function. For the same reason we were not able to measure the refractive index. The best optical properties were demonstrated for the samples with  $R = 15$ , 32 and 50.

*Acknowledgment* – The authors gratefully acknowledge the support from the State Committee for Scientific Research (KBN), Poland under the grant No. 8 T11E 037 19.

## References

- [1] WONG P., *Methods in the Physics of Porous Media*, Academic Press, London 1999, pp. 17–38.
- [2] REISFELD R., JORGENSEN C.K. [Eds.], *Chemistry, spectroscopy and applications of sol-gel glasses* [In] *Structure and Bonding*, Vol. 77, Springer, Berlin 1992.
- [3] JORGENSEN C.K., REISFELD R. [Eds.], *Optical and electronic phenomena in sol-gel glasses and modern application* [In] *Structure and Bonding*, Vol. 85, Springer, Berlin 1996.
- [4] ABRAMOFF B., KLEIN L.C., Proc. SPIE **1328** (1990), 241.
- [5] KLEIN L.C. [Ed.], *Sol-Gel Optics: Processing and Applications*, Kluwer Academic Publishers, Boston 1994.
- [6] BRINKER C.J., SCHERER G.W., *Sol-Gel Science: the Physics and Chemistry of Sol-Gel Processing*, Academic Press, San Diego 1990.
- [7] NICOLAI T., DURAND D., *Scattering Properties and Modeling of Aggregating and Gelling System in Light Scattering*, [Ed.] W. Brown, Clarendon Press, Oxford 1996, pp. 201–231.
- [8] DEBYE P., BUECHE A., J. Appl. Phys. **20** (1949), 518.
- [9] FUKUNAGA K., *Introduction to Statistical Pattern Recognition*, 2nd edition, Academic Press, New York 1990.
- [10] AXLER S., *Linear Algebra Done Right*, Springer-Verlag, New York 1995.
- [11] EVERITT B.S., *Cluster Analysis*, 3rd edition, Edward Arnold, London 1993.
- [12] GU Z.H., LEE S.H., Opt. Eng. **23** (1984), 727.
- [13] ETEMAND K., CHELLAPPA R., J. Opt. Soc. Am. A **14** (1997), 1724.
- [14] GORDON A.D., *Classification: Methods for the Exporatory Analysis of Multivariate Data*, Chapman and Hall, London 1980.
- [15] MCLACHLAN G.J., Statistical Methods in Medical Research **1** (1992), 27.

Received September 26, 2002